Korean J. Chem. Eng., 33(4), 1220-1231 (2016)
DOI: 10.1007/s11814-015-0249-x

pISSN: 0256-1115
eISSN: 1975-7220

Production of a biodiesel additive in a stirred basket reactor using immobilized lipase: Kinetic and mass transfer analysis

Mohamad Hajar and Farzaneh Vahabzadeh†

Department of Chemical Engineering, AmirKabir University of Technology (Tehran Polytechnic), 424 Hafez Avenue, Tehran, Iran

(*Received 8 September 2015 • accepted 17 November 2015*)

Abstract−A laboratory-scale stirred basket reactor (SBR) was constructed to study the synthesis of an n-butyl oleate ester using Novozym 435. An ester yield of approximately 98% was obtained after 6 h using an equimolar substrate ratio, 3.5 g of enzyme, a reaction temperature of 40 °C, and an impeller speed of 200 rpm. The kinetic data were modeled as a ping-pong bi-bi mechanism using a non-linear regression technique. Statistical analysis of the results showed that a model that incorporated the inhibitory effect of n-butanol yielded the best fit with the following parameters: V_{max}=24.8 mmol L^{-1} min^{-1}, $K_{m,\,oleic\,acid}$=190.8 mM, $K_{m,\,n\text{-}butanol}$=544.7 mM, and $K_{i,\,n\text{-}butanol}$=158.3 mM. Mass transfer effects on the enzyme kinetics were also studied, and the absence of internal and external diffusion limitations on the reaction in the SBR was confirmed by considering calculated values of the Thiele modulus and the Damkohler number. Novozym 435 exhibited satisfactory performance in repeated-batch experiments using SBR.

Keywords: Stirred Basket Reactor, Biodiesel Additive, Ester Synthesis, Immobilized Lipase, Kinetic Parameters

INTRODUCTION

Global interest has directed industry towards the use of safer processes that inflict less environmental damage. Direct enzymatic catalysis is the preferred method for converting raw materials to value-added products. Although much attention has been focused on lipases, the use of these enzymes for synthesis is still new and requires more experimental work. Oleochemical esters produced from plant oils and related derivatives have advantages over mineral oil-based products because of their biodegradability and lower toxicity [1-6]. The numerous potential usages of the oleochemical ester n-butyl oleate have directed industrial attention toward this compound. For example, this ester can be employed as a diesel additive, a plasticizer, a water-resistant agent, and in hydraulic fluid [7].

A wide variety of biochemical conversions are carried out using immobilized enzymes, and the advantages of this usage are reinforced using an appropriate design of bioreactor (stirred tank, fluidized bed, packed bed, membrane, etc.). Among these designs, which possess different geometrical characteristics, the packed bed reactor has gained popularity, but the reactor suffers from major weaknesses: laminar flow inside the fixed bed causes low rates of mass and heat transfer; effluent particles may clog the bed; and undesirable channeling may occur inside the bed. Moreover, the widespread use of the stirred tank reactor does not rule out the occurrence of undesirable effects of stirring (i.e., sensitive enzymes respond to shear forces and the mechanical disruption of the biocatalyst particles would be very likely) [8].

Reactor design with respect to reaction kinetics has been described in the literature, and the stirred basket reactor (SBR), in which the baskets are filled with catalyst particles, has been deemed suitable for conducting heterogeneous catalysis experiments. The most salient feature of this reactor configuration is that the high relative velocities between the particles and the surrounding fluid provided by the high-speed rotating basket markedly reduce the external mass transfer resistance. This mixing behavior also reduces the likelihood of non-uniformity in the reaction medium occurring in the axial or radial position. However, internal mass transfer effects are still present in such a system. By using small catalyst particles and/or by maintaining a low rate of conversion, it is possible to overcome these limitations [9,10]. Therefore, the catalyst particles make good contact with the substrate molecules because of adequate mixing in the SBR, enhancing the hydrodynamics associated with the behavior of the liquid phase. For biocatalytic processes in which an immobilized enzyme is employed, enzyme integrity will likely be retained and structural disruption avoided with the use of an SBR.

The catalytic synthesis of n-butyl oleate using Novozym 435 was investigated in this study by constructing and operating a laboratory-scale SBR. The effect of certain operative factors on the reaction rate was quantified for this novel reactor design. These factors were the impeller speed, the amount of enzyme, the temperature, and the molar ratio of the substrates. A kinetic model with substrate inhibition was used to describe the reaction mechanism, and the kinetic constants were determined based on statistical analysis. The effects of mass transfer resistance on the synthesis of the ester were also evaluated.

MATERIALS AND METHODS

1. Materials

Novozym 435 is a commercial immobilized lipase B from *Can-*

†To whom correspondence should be addressed.
E-mail: far@aut.ac.ir

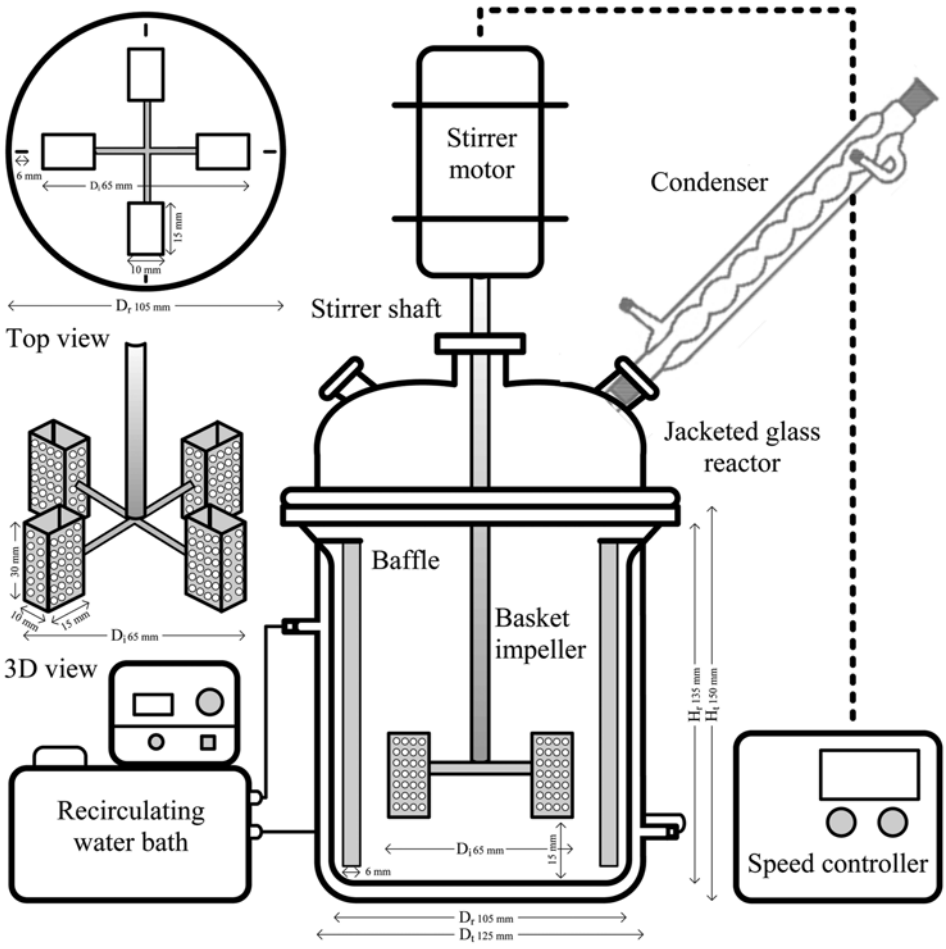

Fig. 1. Schematic diagram of the stirred basket reactor system.

dida antarctica supported on a macroporous acrylic resin and was provided as a gift from Novozymes A/S (Denmark-Tehran office). The physical characteristics of Novozym 435 are as follows: bead size 0.3-0.9 mm, surface area 80 m^2 g^{-1}, and bulk density 0.42 g mL^{-1}. Oleic acid (extra pure) was obtained from the Loba Chemie Co. The Merck Chemical Co. supplied n-butanol (≥99%) and n-hexane. All the other chemicals and reagents were of analytical grade.

2. Reactor Construction and Experimental Setup

The stirred basket reactor used in the present study consisted of a jacketed cylindrical glass vessel with an inner diameter of 105 mm and an inner height of 135 mm (Fig. 1). The basket impeller was fabricated from perforated stainless steel and attached to a central shaft. An appropriate amount of immobilized enzyme (Novozym 435) was filled into each of the four compartments of the basket impeller. The shaft was driven by a variable-speed electric motor, and the system was equipped with a controller (Janke & Kunkel, IKA-WERK, RE166, Staufen, Germany). Four equally spaced baffles were placed inside the reactor, which reduced vortex formation considerably. The temperature of the reactor was controlled by a circulating water bath (WiseCircu WCB-6). The reflux condenser was connected to the reactor to avoid solvent loss.

Enzymatic synthesis of n-butyl oleate was in a batch mode in the SBR in a working volume of 750 mL. The reaction mixture consisted of the substrates oleic acid and n-butanol in an n-hexane medium. The yield of n-butyl oleate ester was dependent on several operational factors: impeller speed, amount of enzyme, reaction temperature, and molar ratio of the substrates. Samples were withdrawn from the reactor at regular time intervals, and the unreacted oleic acid content was determined. Based on these values, the concentration of n-butyl oleate over the reaction time was calculated. At the end of the reaction, the reactor was drained, and the solvent was evaporated under reduced pressure (BUCHI, Rotavapor R-205, Vacuum controller V-800). The ester phase was used for further analysis.

3. Kinetics Studies

Kinetics experiments were carried out in the SBR system by setting the initial concentration of one substrate at a constant level and varying the concentration of the other substrate. Therefore, the series of experiments was designed in a binary matrix in which the oleic acid and the n-butanol concentrations each ranged from 100 to 1,000 mM. For each run, the SBR impeller speed was 200 rpm, the temperature was 40 °C and 3.5 g Novozym 435 was added. Table 1 shows the details of the experimental plan. In this manner, the effects of both substrates on the rate of the enzymatic esterification reaction were described by a ping-pong bi-bi mechanism. Competitive

Table 1. Experimental plan for the modeling kinetics of the n-butyl oleate ester synthesis in the SBR using Novozym 435. The experimental results (mean±SD) and the reaction rates predicted by the model are also shown

Exp. no.[a]	Oleic acid [A] (mM)	n-Butanol [B] (mM)	Initial reaction rate (mmol L^{-1} min^{-1})		
			Experimental	Predicted	Residual
1	100	100	2.75±0.08	2.59	0.16
2	100	200	3.10±0.08	3.08	0.02
3	100	400	2.65±0.07	2.73	−0.08
4	100	600	2.18±0.08	2.24	−0.06
5	100	800	1.82±0.06	1.87	−0.05
6	100	1000	1.55±0.07	1.60	−0.05
7	200	100	3.40±0.14	3.10	0.30
8	200	200	4.41±0.13	4.21	0.20
9	200	400	4.31±0.18	4.33	−0.02
10	200	600	3.78±0.10	3.83	−0.05
11	200	800	3.28±0.08	3.32	−0.04
12	200	1000	2.87±0.13	2.91	−0.04
13	400	100	3.64±0.10	3.43	0.21
14	400	200	5.15±0.14	5.16	−0.01
15	400	400	6.11±0.17	6.13	−0.02
16	400	600	5.97±0.17	5.91	0.06
17	400	800	5.44±0.15	5.43	0.01
18	400	1000	4.89±0.11	4.92	−0.03
19	600	100	3.81±0.11	3.56	0.25
20	600	200	5.39±0.13	5.58	−0.19
21	600	400	6.70±0.11	7.12	−0.42
22	600	600	6.98±0.11	7.22	−0.24
23	600	800	6.94±0.11	6.87	0.07
24	600	1000	6.06±0.15	6.40	−0.34
25	800	100	3.73±0.15	3.63	0.10
26	800	200	5.56±0.15	5.81	−0.25
27	800	400	7.98±0.23	7.74	0.24
28	800	600	8.08±0.23	8.13	−0.05
29	800	800	8.12±0.23	7.93	0.19
30	800	1000	7.90±0.23	7.54	0.36
31	1000	100	3.52±0.15	3.67	−0.15
32	1000	200	5.87±0.17	5.97	−0.10
33	1000	400	8.30±0.24	8.17	0.13
34	1000	600	8.46±0.24	8.78	−0.32
35	1000	800	8.76±0.25	8.74	0.02
36	1000	1000	8.77±0.24	8.43	0.34

[a]For each run, the SBR impeller speed was 200 rpm, the temperature was 40 °C and 3.5 g Novozym 435 was added. The reaction volume was set at 750 mL

inhibition is the focus of this mechanism and is shown in Scheme 1. Considering the inhibition by both substrates, the rate equation is as follows [2,11]:

$$\nu = \frac{V_{max}[A][B]}{[A][B] + K_{mA}[B]\left(1+\frac{[B]}{K_{iB}}\right) + K_{mB}[A]\left(1+\frac{[A]}{K_{iA}}\right)} \quad (1)$$

where ν is the initial rate of the esterification reaction; V_{max} is the maximum rate of the reaction; [A] and [B] are the initial molar concentrations of oleic acid (A) and n-butanol (B), respectively; K_{mA} and K_{mB} are the Michaelis constants; and K_{iA} and K_{iB} are the inhibition constants for oleic acid and n-butanol, respectively.

In the absence of substrate inhibition by oleic acid, Eq. (1) can be modified as follows:

$$\nu = \frac{V_{max}[A][B]}{[A][B] + K_{mA}[B]\left(1+\frac{[B]}{K_{iB}}\right) + K_{mB}[A]} \quad (2)$$

The reaction kinetics for the enzymatic catalysis of two substrates in the absence of an inhibitor has been defined as follows:

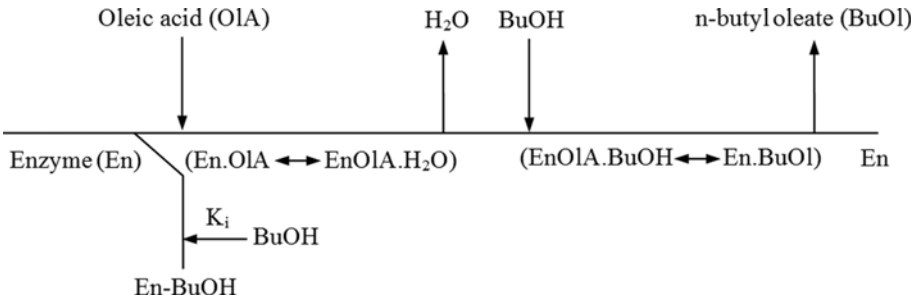

Scheme 1. Ping-pong bi-bi mechanism for the lipase-catalyzed synthesis of n-butyl oleate ester in an SBR.

$$v = \frac{V_{max}[A][B]}{[A][B] + K_{mA}[B] + K_{mB}[A]} \quad (3)$$

The initial reaction rate for each run was determined from the slope of the initial linear portion in the plot of the amount of ester produced versus time. The above-mentioned rate equations were used to calculate the kinetic parameters by considering the experimental data that fit the model by non-linear regression analysis.

4. Analytical Methods

The free fatty acid content in terms of unreacted oleic acid in the test reaction mixture was determined by a colorimetric method [12,13]. Cupric acetate-pyridine reagent was prepared by dissolving 5% (w/v) of cupric acetate in water, and after filtration, the pH of the reagent solution was adjusted to 6.1 by adding pyridine. Samples of the test mixture containing oleic acid were transferred into 15 mL test tubes and dissolved by adding 5 mL of isooctane solvent followed by the addition of 1 mL of cupric acetate-pyridine reagent. The tubes were vortexed vigorously for 90 s, and the solutions were allowed to stand until the contents separated into two phases. The absorbance of the upper phase was measured at 715 nm on a JASCO V-550 spectrophotometer, and the amount of free fatty acid was determined with a standard curve of oleic acid in the range of 5-50 μmol/5 mL isooctane.

Nuclear magnetic resonance (NMR) analyses were performed using a Bruker DRX-500 spectrometer with tetramethylsilane (TMS) as an internal standard. The samples were dissolved in deuterated chloroform ($CDCl_3$) as the solvent. The ^1H and ^{13}C-NMR spectra were recorded at 500 and 125 MHz, respectively.

Further studies characterized the synthesized n-butyl oleate ester according to measurements of its physicochemical properties. The density, kinematic viscosity, acid value, cloud point, pour point, and flash point were determined by using standard procedures described by the American Society for Testing and Materials (ASTM).

5. Statistical Analysis

All experimental runs and samples from the SBR were performed in duplicate, and the mean values±standard deviation (SD) were reported. The SD values were lower than 5%, and the data variability in the relevant graphs is shown as error bars. The kinetic parameters estimated from the experimental results were performed by non-linear regression with a Marquardt-Levenberg algorithm. In this method, the goal is to minimize the sum of squares of the differences between the values predicted by the model and the measured values. All statistical data analyses and non-linear curve fitting were performed using SigmaPlot version 11, Systat Software, Inc.

Tests of statistical significance are based on tests of a hypothesis. The significance of the results is determined when the null hypothesis is rejected. The *p*-value represents the probability of committing a type I error in testing the hypothesis, which is based on a *t*-test and the *F*-ratio (a type I error is defined as a decision made by falsely rejecting a null hypothesis (H_0) when H_0 is true). The smaller the *p*-value is, the greater the probability that the obtained result is significant becomes; *p*-values less than 0.05 were considered indicative of statistical significance [14].

RESULTS AND DISCUSSION

1. Effects of Influential Factors on Ester Synthesis in the SBR

The enzymatic synthesis of n-butyl oleate ester in the SBR was monitored for various impeller speeds ranging from 100 to 250 rpm, and the yield as the function of the reaction time is shown in Fig. 2. The figure inset shows the dependence of the initial reaction rate on the impeller speed. No rate change was observed at speeds above 200 rpm. Increasing the speed of liquid mixing was correlated with the decrease in the size of the dispersed substrate molecules in the bulk phase. Increasing the interfacial area increases

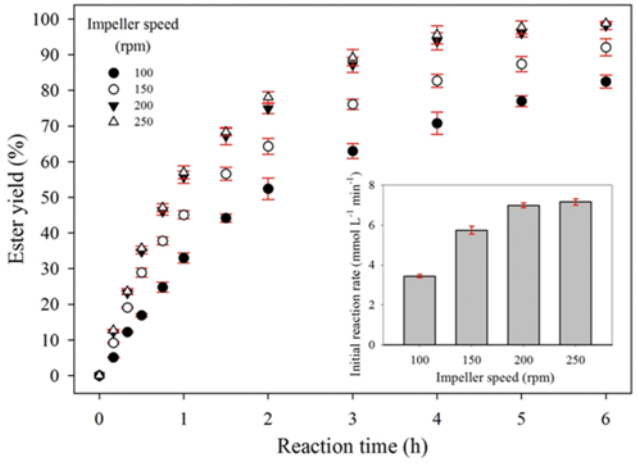

Fig. 2. Effects of the impeller speed on the lipase-catalyzed synthesis of n-butyl oleate ester in the SBR. Reaction conditions: enzyme amount, 3.5 g; temperature, 40 °C; and substrate molar ratio, 1 : 1. The inset shows the initial reaction rate as a function of the impeller speed.

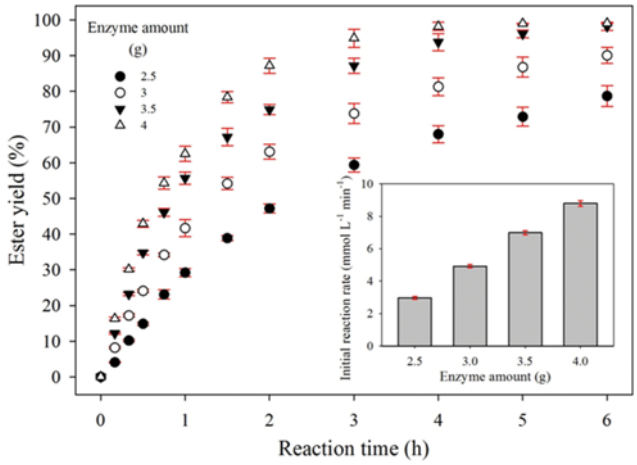

Fig. 3. Effects of the enzyme amount on the lipase-catalyzed synthesis of n-butyl oleate ester in the SBR. Reaction conditions: Impeller speed, 200 rpm; temperature, 40 °C; and substrate molar ratio, 1 : 1. The inset shows the initial reaction rate as a function of the amount of enzyme.

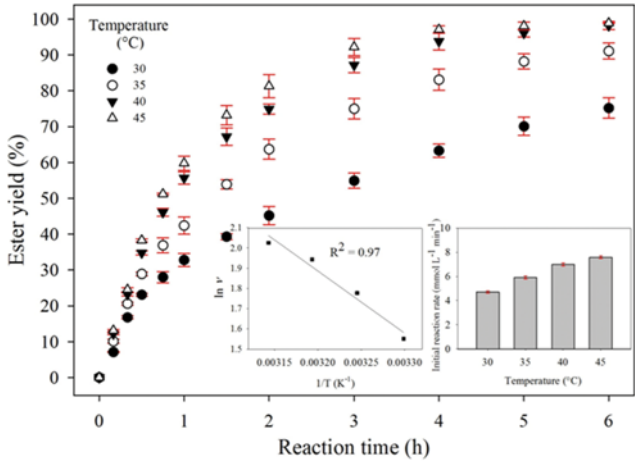

Fig. 4. Effects of temperature on the lipase-catalyzed synthesis of n-butyl oleate ester in the SBR. Reaction conditions: Impeller speed, 200 rpm; enzyme amount, 3.5 g; and substrate molar ratio, 1 : 1. The inset shows the initial reaction rate as a function of the temperature.

the probability of effective collisions between substrate molecules and enzyme particles [15,16]. These observations indicate that mass transfer limitations do not affect ester synthesis at a high mixing speed (>200 rpm). The initial reaction rate of n-butyl oleate synthesis was 6.98 mmol L^{-1} min^{-1} at an impeller speed of 200 rpm. After 4 h of reaction, 94% of the oleic acid was utilized. Further experiments were performed at an impeller speed of 200 rpm.

The rate of the biocatalytic reaction (the enzyme saturation kinetics) is governed by the amount of enzyme. Four different amounts of enzyme ranging from 2.5 to 4 g, with a working volume of 750 mL for the SBR (equivalent to 1.97-3.15 w/w of oleic acid), were used in this study (Fig. 3). The linear dependence of the initial reaction rate on the enzyme amount shown in the inset of Fig. 3 indicates that ester synthesis was kinetically controlled. The rate increased from 2.96 to 8.79 mmol L^{-1} min^{-1} for enzyme levels of 2.5 to 4 g, respectively. The probability of a collision between a substrate and an enzyme in a test solution increases with the amount of enzyme, but the enzyme content does not change the equilibrium position of a reaction; it only reduces the time required to reach equilibrium [1]. The results shown in Fig. 3 indicate that the amount of ester yield did not change considerably beyond 4 h at an enzyme mass greater than 3.5 g (i.e., equilibrium position). Therefore, the experiments were further directed by loading 3.5 g of Novozym 435 into the basket compartment of the impeller.

Fig. 4 shows that an increase in the reaction temperature from 30 to 45 °C increased the initial reaction rate from 4.71 to 7.58 mmol L^{-1} min^{-1}. The highest yield of the ester (96%) was obtained after 5 h at 40 °C, and no difference in the yield at 45 °C was observed. The dependence of the reaction rate (ν) on temperature (T) was determined according to the Arrhenius equation [9]:

$$\ln \nu = \frac{-E_a}{R}\left(\frac{1}{T}\right) + \ln A \quad (4)$$

The value of the activation energy (E_a) was calculated to be 25.6 kJ mol^{-1}. The frequency factor (A) in the equation is defined as the reaction rate parameter at a given temperature. In fact, the collision frequency is affected by the concentration of the reactant molecules and the rapidity of the movement of these molecules, the kinetic energy of which depends on temperature. Considering that proteins have a marginally stable structure in their native state, increasing the reaction temperature beyond a certain level negatively affects enzyme functionality (i.e., enzyme inactivation) [16,17]. The synthesis of n-butyl oleate ester in n-hexane was examined in a previous study using nylon-immobilized lipase from *Candida rugosa*, in which the reported E_a value was 37 kJ mol^{-1} [18]. In another study, Novozym 435 was used for the catalytic synthesis of cinnamyl acetate in non-aqueous medium, in which the activation energy was 27.2 kJ mol^{-1} [19]. The preferred role of Novozym

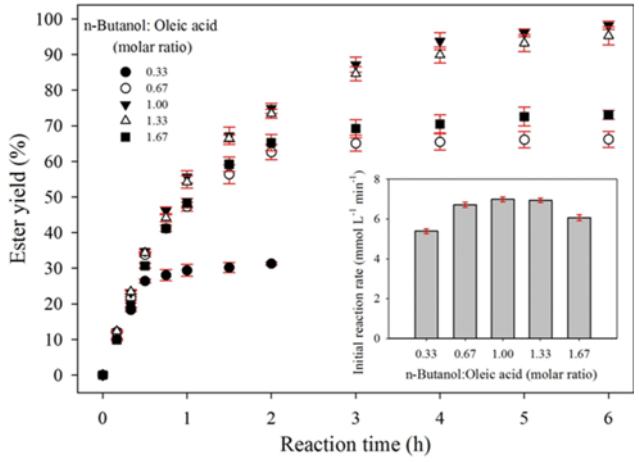

Fig. 5. Effects of the substrate molar ratio on the lipase-catalyzed synthesis of n-butyl oleate ester in the SBR. Reaction conditions: Impeller speed, 200 rpm; enzyme amount, 3.5 g, and temperature, 40 °C. The inset shows the initial reaction rate as a function of the substrate molar ratio.

435 in the SBR in the present study can be determined by comparing these E_a values.

The molar ratio of n-butanol to oleic acid was varied from 0.33 to 1.67 at a constant concentration of oleic acid (600 mM) to study the effect of the substrate on the yield of the ester and the reaction rate. As shown in the inset of Fig. 5, the initial reaction rate increased with the molar ratio up to an equimolar concentration of the test alcohol and fatty acid substrates. At this point, the highest ester yield of approximately 98% was obtained after 6 h. The reaction did not advance at a molar ratio greater than 1.33. This decreasing trend can be attributed to the relationship between lipase and alcohol during the ester synthesis, which could be quantified by considering the substrate inhibition effect. In other words, the inactive complex that is usually formed between the lipase and alcohol is a type of barrier (or dead-end complex) to the continuation of the reaction that has been well described in the literature in terms of ester synthesis [18,20]. Hydrogen bonding of alcohol, which has hydrophilic characteristics, might lead to the exclusion of water from the enzyme microenvironment; thus, the sensitivity of the enzyme to natural denaturation increases markedly [7]. Thus, the adjacent alcohol molecules are a real barrier to the diffusion of the enzyme towards oleic acid, which is a hydrophobic substrate.

The Pearson's correlation coefficient (r) used in the present study only indicates the strength of the linear relationship between the test variables. So, even in the absence of this relationship (r=0), the possibility of a curvilinear relationship between the variables cannot be ruled out [21]. According to the results shown in the insets of Figs. 2-5, the values of r are as follows: r=1 for enzyme amount, r=0.99 for temperature, r=0.93 for impeller speed, and r=0.37 for substrate molar ratio. The low value of r for the latter case cannot exclude the presence of a non-linear relationship between the substrate molar ratio and initial reaction rate.

2. Mass Transfer Effects

An assessment of a reactor's performance actually depends on both the reaction kinetics and the mass transfer limitations of the biocatalytic process. The extent of the latter could be reduced by carrying out the bioprocess close to the intrinsic properties of the biocatalyst. Fluctuations in substrate/product concentrations during a reaction are indicative of molecular transfer resistance that occurs between the bulk and the surface of the biocatalyst (i.e., the interparticle diffusion effect or external mass transfer). Diffusion of the substrate/product molecules within the biocatalyst is indicative of mass transfer limitations inside the catalyst (i.e., the intraparticle diffusion effect or internal mass transfer) [22].

The external mass transfer effect was determined by calculating the solid-liquid mass transfer coefficient (K_{SL}) [9]:

$$\mathrm{Sh}=2+0.6\mathrm{Re}_p^{0.5}\mathrm{Sc}^{0.33} \tag{5}$$

The correlation was defined by the following dimensionless numbers [9]:

$$\mathrm{Re}_p\ (\text{Reynolds number})=\frac{\mathrm{D}_p\mathrm{u}_{pL}\rho_L}{\mu_L} \tag{6}$$

$$\mathrm{Sc}\ (\text{Schmidt number})=\frac{\mu_L}{\rho_L\mathrm{D}_{AL}} \tag{7}$$

$$\mathrm{Sh}\ (\text{Sherwood number})=\frac{\mathrm{K}_{SL}\mathrm{D}_p}{\mathrm{D}_{AL}} \tag{8}$$

where D_p is the particle diameter (cm), which is equal to 0.06 for Novozym 435; u_{pL} is the particle velocity relative to the bulk liquid (cm s^{-1}); and ρ_L and μ_L are the density (g cm^{-3}) and the viscosity of test liquid mixtures (g $cm^{-1}s^{-1}$), respectively. The value of the oleic acid diffusivity in n-hexane (D_{AL}, cm^2 s^{-1}) was determined according to the Wilke-Chang expression [23]:

$$\mathrm{D}_{AL}=7.4\times10^{-8}\frac{\mathrm{T}(\mathrm{xM})^{1/2}}{\eta\mathrm{V}_s^{0.6}} \tag{9}$$

where T is the absolute system temperature in Kelvin, M is the molecular weight of the solvent (g mol^{-1}) and η is the solvent viscosity (cP). The association factor of the solvent (x) is equal to 1 for n-hexane as an unassociated liquid. The molar volume of the solute at the normal boiling point (V_s, cm^3 mol^{-1}) is determined using the Tyn-Calus equation [24]:

$$\mathrm{V}_s=0.285\times\mathrm{V}_c^{1.048} \tag{10}$$

where V_c is the critical volume of oleic acid estimated by the Joback-Reid method (V_c=1047.5 cm^3 mol^{-1}) [25]. By setting V_s equal to 416.8 cm^3 mol^{-1}, the diffusivity of oleic acid can be determined using Eq. (9) (D_{AL}=2.1587×10^{-5} cm^2 s^{-1}). At this stage, using the concentrations of the reaction components (oleic acid and n-butanol in n-hexane solvent) given in Table 1, the two dimensionless numbers Re and Sc were determined (Eqs. (6) and (7)), and the Sherwood number was then computed using Eq. (5). Subsequently, the mass transfer coefficient, K_{SL}, was determined using Eq. (8); the value ranged from 1.89×10^{-2} to 2.21×10^{-2} cm s^{-1}. These coefficients allowed for the determination of the Damkohler number (Da is the observable value of this dimensionless number) to quantitatively describe the external mass transfer effects [22]:

$$\mathrm{Da}=\frac{\nu}{\mathrm{K}_{SL}\mathrm{a}_c\mathrm{S}_0} \tag{11}$$

where ν is the initial reaction rate, a_c is the external surface area to volume of the biocatalyst and S_0 is the initial substrate concentration (i.e., oleic acid). The values of Da ranged from 0.3×10^{-4} to 2.3×10^{-4}; therefore, the mass transfer resistances were not notable. To compare the mass transfer rate to the reaction rate, the external effectiveness factor (η_E) was used [26]:

$$\eta_E=\left[\frac{1}{2\mathrm{Da}}\left(\sqrt{1+4\mathrm{Da}}-1\right)\right] \tag{12}$$

Because the value of η_E lies between 0.9997 and 0.9999 for the experiments specified in Table 1, the external mass transfer effects were unimportant in this study.

The occurrence of internal mass transfer diffusion was evaluated by determining the Thiele modulus (Φ is the observable value of this dimensionless number) [22]:

$$\Phi=\frac{\nu}{\mathrm{D}_E\mathrm{S}_0}\left(\frac{\mathrm{V}_p}{\mathrm{A}_p}\right)^2 \tag{13}$$

where D_E is the effective diffusivity of the substrate within the catalyst pores (cm^2 s^{-1}) and V_p and A_p are the volume (cm^3) and the

surface area (cm^2) of the catalyst particles, respectively. Assuming that Novozym 435 is spherical, the following expression can be used to determine Φ [22]:

$$\Phi = \frac{\nu}{D_E S_0}\left(\frac{R_p}{3}\right)^2 \quad (14)$$

The catalyst particle porosity (ε_p), tortuosity (τ), and the constriction factor (σ_c) are all important in quantifying the value of D_E:

$$D_E = \frac{D_{AL}\varepsilon_p\sigma_c}{\tau} \quad (15)$$

The values of ε_p, τ, and σ_c for Novozym 435 are 0.5, 6, and 1, respectively [27]; thus, D_E was estimated to be 1.7989×10^{-6} cm^2 s^{-1}. Thereafter, Φ was determined to range from 0.0033 to 0.0287 during the experimental runs shown in Table 1. These small values of Φ indicate that intraparticle diffusion was negligible. Moreover, the following expression can be used to describe the internal effectiveness factor (η_I) in terms of the Φ index [22]:

$$\eta_I = \frac{1}{\phi}\left(\frac{1}{\tanh 3\phi} - \frac{1}{3\phi}\right) \quad (16)$$

The values of η_I are range from 0.9995 to 0.9999. All of these calculations indicate that the reaction is kinetically controlled.

3. Kinetic Modeling

Scheme 1 graphically presents the ping-pong bi-bi mechanistic model described for the lipase-catalyzed reaction in which the n-butyl oleate ester was synthesized using n-butanol and oleic acid substrates. The binding of lipase to the oleic acid and the formation of the acyl-enzyme complex (E.OlA) is coupled to the relevant isomerization with the concomitant release of the first product (water). With n-butanol as the second substrate, the transformation continues through formation of a binary complex: the combined form of the acyl-enzyme with the alcohol (EOlA.BuOH). The reaction progresses with the isomerization of the tertiary complex and the associated release of the n-butyl oleate ester as the second product. The regeneration of the enzyme completes the catalytic cycle, and the catalysis can be continued by further reaction with E, OlA, and BuOH [18,28].

To kinetically model a reaction with two substrates requires sets of experiments in which the concentration of one substrate is varied while that of the other is held constant, as presented in Table 1. Lineweaver-Burk plots of the reciprocal of the initial reaction rate versus the reciprocal of the oleic acid and n-butanol substrate concentrations are shown in Fig. 6. The applicability of the ping-pong bi-bi mechanism is clearly evident at low concentrations of butyl alcohol (i.e., parallel lines on the double reciprocal plot) (Fig. 6(b)). However, at high levels of n-butanol (low values of reciprocal of the alcohol concentration), the lines in the plot are concave upward, which is indicative of alcoholic inhibition. Fig. 6(a) indicates no inhibition with oleic acid as a substrate.

Eqs. (1)-(3) were derived based on the fundamental concept of the catalytic reaction with two substrates, and the kinetic parameters were determined using a non-linear regression technique (Marquardt-Levenberg algorithm). The strategy for parameter calculation in this algorithm is to find the lowest value for the residual sum of squares (RSS), which is used as an index for the ability

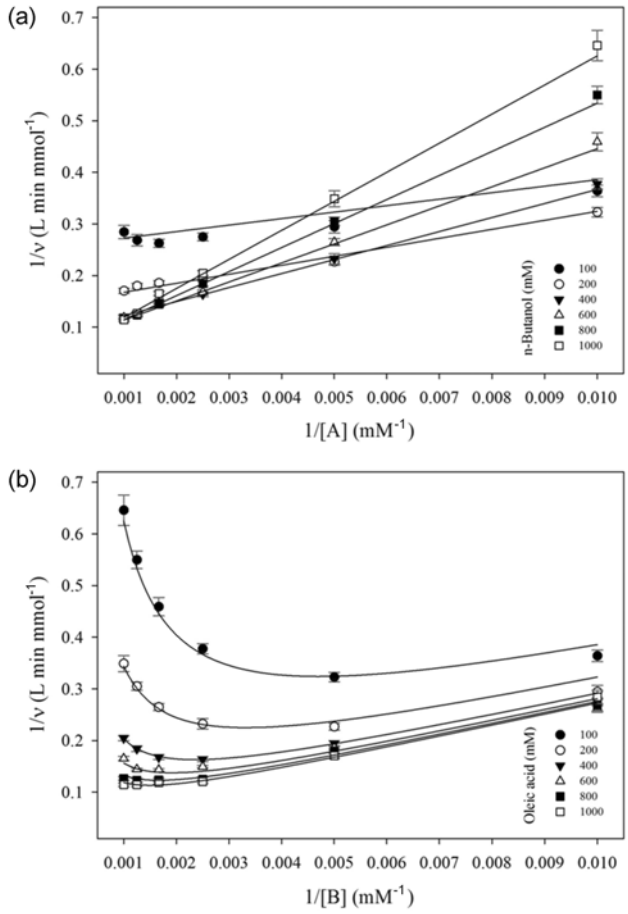

Fig. 6. Double-reciprocal plot of the initial reaction rate of the enzymatic synthesis of n-butyl oleate as a function of the oleic acid concentration at the fixed levels of n-butanol (a) and as a function of the n-butanol concentration at fixed levels of oleic acid (b). The solid lines represent the corresponding values predicted by the model.

of the model to estimate the experimental data. The iterative curve fitting process employed by the software converges when no further changes are observed for the differences between the RSS values. The results of the model comparison are presented in Table 2. The independence of the kinetics coefficients was determined by using the *t*-statistic, which has been defined as the ratio of the coefficient to the relevant standard error. The relationship between the *t*-statistic and *p*-value further shows that K_{iA}, as the inhibition constant for oleic acid, could be removed from the model presented in Eq. (1) (*t*-statistic<2 corresponding to a *p*-value>0.05) (Table 2(a)) [14]. Eq. (2) was applied without the K_{iA} term, and the variance constancy test confirmed the adequacy of the model (Eq. (2)). Further statistical tests with the least squares technique were performed to evaluate the random error (i.e., the difference between the experimental data and the data predicted by the model), and the Durbin-Watson statistic was used to measure the correlation between the residuals to determine the independence of the error [29]. A value of 1.946 for model Eq. (2) is approximately equal to 2; therefore, one may conclude that the residuals are independent (Table 2(d)). A normal distribution of the source popula-

Table 2. Statistical analysis of the data obtained using a non-linear regression technique for selecting the kinetic model: (a) Kinetic parameters obtained for the three different models, (b) ANOVA for the fitted model according to the reaction mechanism, (c) statistical parameters used to determine the model's adequacy, and (d) statistical tests used to evaluate the regression assumptions

	Inhibition by both substrates (Eq. (1))				Inhibition by the alcohol substrate (Eq. (2))				No substrate inhibition (Eq. (3))			
a) Kinetic constants	Coefficient	Std. error	*t*-test	*P*-value	Coefficient	Std. error	*t*-test	*P*-value	Coefficient	Std. error	*t*-test	*P*-value
V_{max} (mmol L^{-1} min^{-1})	26.4226	2.152	12.278	<0.0001	24.7925	1.687	14.692	<0.0001	15.4431	1.546	9.986	<0.0001
K_{mA} (mmol L^{-1})	265.4487	60.547	4.384	0.0001	190.8157	37.736	5.057	<0.0001	561.5228	103.733	5.413	<0.0001
K_{mB} (mmol L^{-1})	509.2119	58.625	8.686	<0.0001	544.7422	55.769	9.768	<0.0001	186.5293	38.339	4.865	<0.0001
K_{iA} (mmol L^{-1})	5478.6055	3542.92	1.546	0.1322	----	----	----	----	----	----	----	----
K_{iB} (mmol L^{-1})	210.9328	53.246	3.962	0.0004	158.2968	41.194	3.843	0.0005	----	----	----	----
b) Source of variation	DF SS	MS	*F*-ratio	*P*-value	DF SS	MS	*F*-ratio	*P*-value	DF SS	MS	*F*-ratio	*P*-value
Regression	4 163.621	40.905	1111.34	<0.0001	3 163.509	54.503	1391.77	<0.0001	2 151.365	75.683	186.425	<0.0001
Residual	31 1.141	0.037			32 1.253	0.039			33 13.397	0.406		
Total	35 164.762	4.707			35 164.762	4.707			35 164.762	4.707		
c) Statistical parameters												
Rsqr	0.9931				0.9924				0.9187			
Adj Rsqr	0.9922				0.9917				0.9138			
Standard error of estimate	0.1919				0.1979				0.6372			
d) Statistical test												
Durbin-Watson statistic	Passed (1.8628)				Passed (1.9458)				Failed (0.9819)			
Normality test (Shapiro-Wilk)	Passed (P=0.1229)				Passed (P=0.4969)				Passed (P=0.7503)			
Constant variance test	Failed (P=<0.0001)				Passed (P=0.0806)				Passed (P=0.0758)			

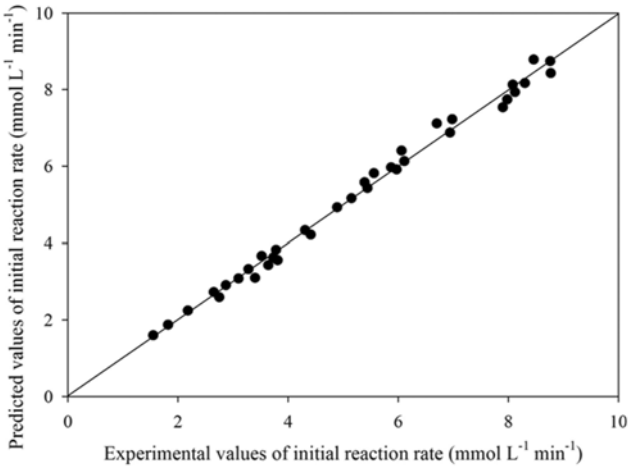

Fig. 7. Parity plot of the initial reaction rates and model-predicted values based on a ping-pong bi-bi mechanism with inhibition by the alcohol substrate.

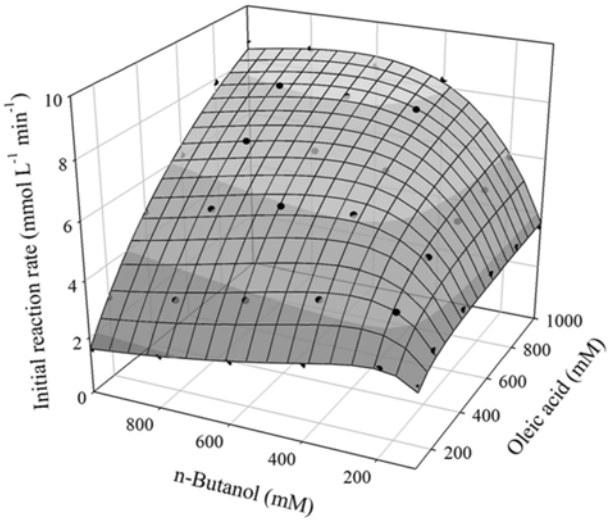

Fig. 8. Three-dimensional plot of the developed model (ping-pong bi-bi kinetics with alcohol substrate inhibition) showing the dependence of the initial reaction rate on the concentration of oleic acid and n-butanol and their interactions.

tion around the regression line was assumed for the residual quality. The normality test did not fail (Table 2(d)). The fit of the experimental data to the model (Eq. (2)) was satisfactory, as shown in the relevant parity plot (Fig. 7). Table 2(c) indicates that the values of R^2 and the standard error of the estimate (SSE) about the regression for Eq. (2) are 0.992 and 0.198, respectively. The decrease in the R^2 value and the SSE for the model given by Eq. (3) suggests that the Eq. (3) model is inadequate. All of this information indicates that the model described by Eq. (2) better describes the enzymatic reaction, in which the inhibitory action of the alcoholic substrate (n-butanol) is incorporated into the model.

A key issue associated with an enzymatic reaction involving two substrates is the affinity of the enzyme for a substrate, where K_m is defined as the half-saturation constant and the substrate with the lower K_m value is the preferred substrate for the formation of the enzyme-substrate complex [30,31]. According to the K_m values shown in Table 2, oleic acid has a higher affinity for Novozym 435 than does n-butanol ($K_{mA}<K_{mB}$). This finding agrees with the illustration shown in Scheme 1. K_i is the inhibition constant, another important biokinetic parameter that measures the sensitivity of the reaction system to inhibition by a particular substance. The inhibitory behavior of the alcoholic substrate n-butanol negatively affects the progress of the reaction because its binding to the enzyme (i.e., dead-end complex) prevents the transfer of the acyl group of oleic acid and the complexation of oleic acid to the enzyme (Scheme 1).

The reported values for the $K_{m,\,oleic\,acid}$, $K_{m,\,ethanol}$, and $K_{i,\,ethanol}$ constants in the formation of ethyl oleate ester in n-hexane using Lipozyme (from *Mucor miehei*) are 120, 190, and 40 mM [28]. Comparisons between these values and the values obtained in the present study show that Novozym 435 in the SBR was more effective in response to the alcoholic substrate, and n-butanol appears to have been less inhibitory in the synthesis of n-butyl oleate ester. In another study in which nylon-immobilized lipase (*Candida rugosa*) was used in the formation of n-butyl oleate in n-hexane, the reported values of K_{mA} and K_{mB} were 380 and 190 mM, respectively [18]. Comparison between the values of the half-saturation constants shows that Novozym 435 in the SBR exhibited a higher affinity towards the oleic acid substrate.

Based on the ping-pong bi-bi mechanism and the inhibitory action of n-butanol, a three-dimensional plot of the kinetic model is shown in Fig. 8. At a low concentration of oleic acid, the reaction rate initially increases to a peak with an increasing concentration of n-butanol; then, a further increase in the n-butanol concentration causes a decrease in the reaction rate. The lowest initial reaction rate (1.55 mmol L^{-1} min^{-1}) corresponds to the highest n-butanol concentration (1,000 mM) and the lowest oleic acid concentration (100 mM) (Fig. 8 and Table 1). The reaction rate becomes constant after a certain point with an increase in the oleic acid concentration, with a simultaneous increase in the n-butanol concentration. The maximum initial reaction rate of 8.77 mmol L^{-1} min^{-1} was obtained at an equimolar concentration of each substrate (1,000 mM) (Fig. 8).

4. Repeated Batches in the SBR

The effectiveness of enzyme utilization in a reaction is well described by enzyme reusability, and the major economic concern in the commercialization of these types of reactions is the stability of the process. The conditions used to test the repeated use of Novozym 435 in the SBR were as follows: an impeller speed of 200 rpm, an enzyme mass of 3.5 g, a temperature of 40 °C, and an n-butanol to oleic acid molar ratio of 1 : 1. After a 6 h reaction cycle, all of the reactor contents were drained from the SBR except for the biocatalyst. After the enzyme was washed with n-hexane, the reaction cycle was renewed using a fresh reaction mixture, and this procedure was repeated for ten cycles. The ester yield obtained for the first cycle was 98% and decreased to 87% after ten cycles. The findings show that the performance of the SBR is suitable for industrial application.

5. Product Characterization Using NMR Analyses

The relative positions of the hydrogen and carbon atoms in the synthesized n-butyl oleate ester were determined by NMR spectroscopy, and the structure of the ester molecule was confirmed.

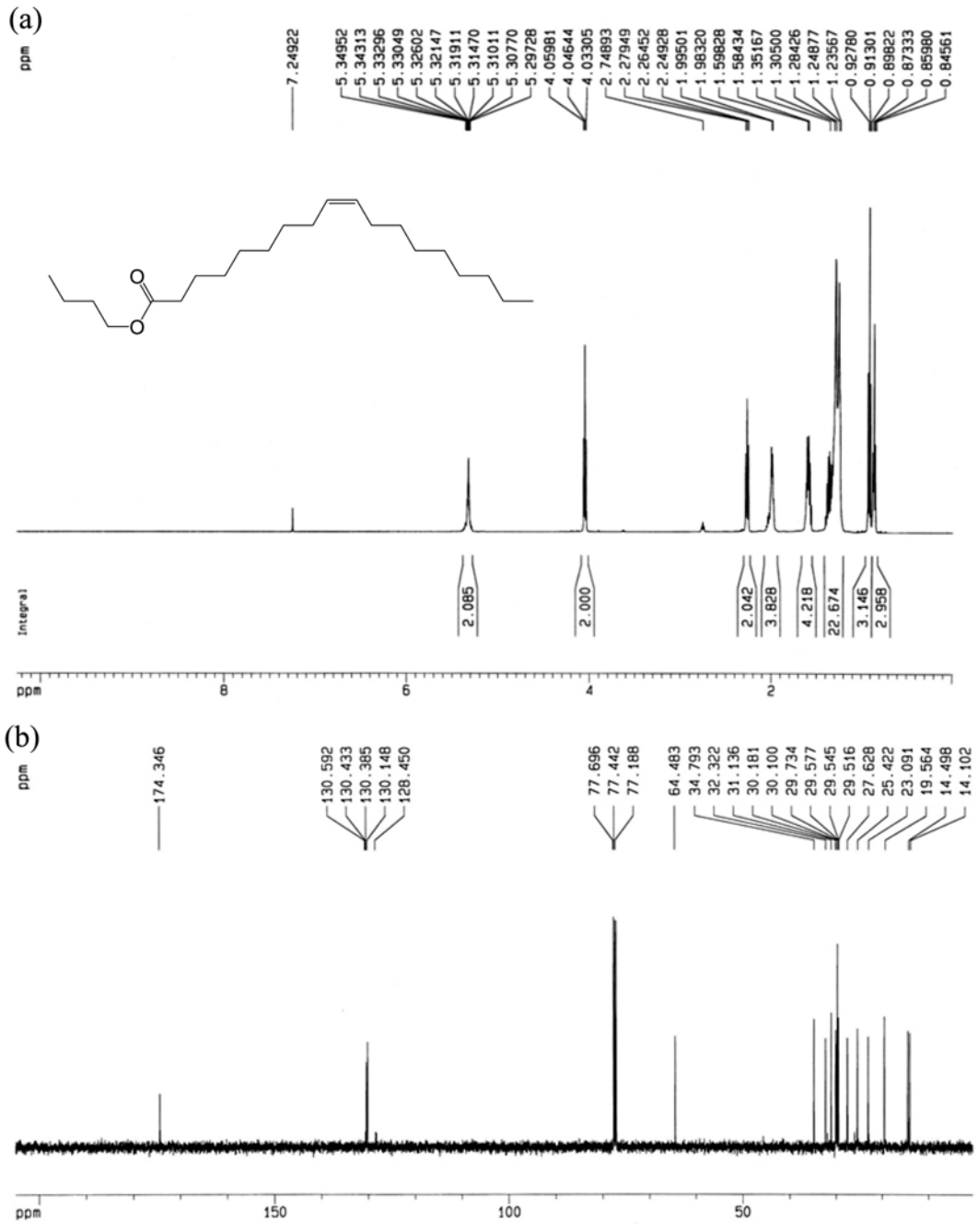

Fig. 9. ^{1}H (a) and ^{13}C (b) NMR spectra of the ester synthesized by the enzymatic esterification reaction of oleic acid and n-butanol.

The ^{1}H-NMR spectrum is shown in Fig. 9(a). Compared to the ^{1}H-NMR spectrum of oleic acid presented in the literature [32], the appearance of a strong triplet peak at 4 ppm revealed that protons from the methylene carbon of n-butanol participated in an ester linkage with the carbonyl group of oleic acid (i.e., -CO-O-CH_2- characteristic of n-butyl oleate). A multiplet signal at 5.3 ppm indicates olefinic protons (-CH=CH-) in the ester product. The triplet signal at 2.3 ppm was assigned to protons from the α-carbonyl methylene group (-CH_2-CO-O-). The methylene group protons located on the carbon atom adjacent to the double bond (allylic protons) show a signal at 2 ppm. The signals at 1.6 ppm indicate protons from two methylene groups, one at the β-position of the carbonyl group and the other one at the second carbon of the alcoholic chain. The signals at 0.9 ppm are characteristic of terminal methyl group protons located at both ends of the n-butyl oleate ester molecule. The signals at 1.2-1.4 ppm are attributed to the other protons in the methylene groups of the ester molecule.

A ^{13}C-NMR spectrum is also presented in Fig. 9(b), and a comparison was made with a ^{13}C-NMR of oleic acid before esterification. The appearance of a new peak at 64 ppm indicates a methylene group carbon attached to the oxygen atom next to the carbonyl group of the ester molecule. The signals at 14 ppm are associated

Table 3. Physicochemical properties of n-butyl oleate ester synthesized in the SBR

Property	Unit	Test method	Result
Kinematic viscosity at 40 °C	$mm^2\ s^{-1}$	ASTM D-445	6.2
Kinematic viscosity at 100 °C	$mm^2\ s^{-1}$	ASTM D-445	2.2
Viscosity index	---	ASTM D-2270	196
Density at 15 °C	$g\ cm^{-3}$	ASTM D-4052	0.868
Acid value	mg KOH g^{-1}	ASTM D-664	0. 5
Pour point	°C	ASTM D-97	−21
Cloud point	°C	ASTM D-2500	−15
Flash point	°C	ASTM D-93	185
Refractive index at 25 °C	---	ASTM D-1747	1.4470

with the terminal methyl groups at both ends of the ester molecule. The peak at 174 ppm was assigned to the carbonyl group carbon. The signal that appeared at 130 ppm was assigned to olefinic carbons. The remaining signals at 19-34 ppm are related to the methylene carbons of the long carbon chain of the ester molecule.

6. Physicochemical Characteristics of the Synthesized Ester

The potential application of esters as biolubricants or fuel additives greatly depends on their physicochemical characteristics, and Table 3 shows some properties of the n-butyl oleate ester synthesized in this study. The protective role of a lubricant is related to its ability to reduce friction and wear and depends on viscosity [33]. Viscosity tests were conducted at different temperatures (40 and 100 °C) to determine viscosity index (VI) and thereby evaluate the variation of the kinematic viscosity as a function of temperature. The viscosity index for the ester synthesized in this study was 196 (Table 3). This high VI is a measure of the strength of the intermolecular forces in the molecule and indicates a high-performing lubricant because of its low sensitivity to temperature fluctuations [1,33]. Density is important in combustion systems in which the flow of fuel into the engine affects fuel atomization and distribution. The density of the synthesized ester was 0.868 g cm^{-3}. Another characteristic of fuel is the free fatty acid (FFA) content, and a high value of FFA indicates fuel aging. It is desirable to use an ester with a zero FFA content as a fuel additive. The acid value for the ester product in this study was low (0.5 mg KOH g^{-1}). The cloud point (CP) and pour point (PP) are important characteristics for fuel used at low temperatures. The CP is the temperature at which haziness first becomes visible, whereas the PP indicates the lowest temperature at which movement of liquid fuel is observable [1]. The CP and PP values for the ester synthesized in this study were −15 and −21 °C, respectively (Table 3). The low values of these characteristics of the fuel additive are desirable, and the likelihood that the fuel can be used at low temperature is high. Volatilization of a lubricant at high temperature represents a weakness and decreases safety [3,33]. Thus, a lubricant that has a high flash point (FP) is desirable; in fact, the FP of the ester synthesized in this study was high (FP=185 °C).

CONCLUSIONS

The successful application of a laboratory-scale SBR for the synthesis of an n-butyl oleate ester using Novozym 435 has been reported. The reaction progress was markedly affected by certain operating factors, such as the impeller speed. The study of reaction restrictions caused by mass transfer resistance indicated that a good mixing design in the SBR reduced these limitations. The ping-pong bi-bi mechanism was used to model the kinetics of the reaction. Statistical comparisons of the test model showed that reaction with n-butanol as an inhibitor was preferable. Batch experiments were repeated for ten cycles without significant loss of enzyme activity, indicating the reusability potential of Novozym 435. Data pertaining to the physicochemical characteristics of the n-butyl oleate ester indicate that the ester can be applied in a wide range of products, such as lubricants and diesel fuel additives. The results obtained in this study can be useful in the design and operation of industrial-scale reactors for the enzymatic synthesis of oleochemical esters.

NOMENCLATURE

[A] : initial molar concentration of oleic acid (A) [mmol L^{-1}]
A_p : surface area of catalyst particle [cm^2]
A : frequency factor or pre-exponential factor
a_c : external surface area to volume of the biocatalyst [$cm^2\ cm^{-3}$]
[B] : initial molar concentration of n-butanol (B) [mmol L^{-1}]
Da : Damkohler number
D_{AL} : diffusivity of oleic acid in n-hexane [$cm^2\ s^{-1}$]
D_E : effective diffusivity of substrate within catalyst pores [$cm^2\ s^{-1}$]
D_p : particle diameter [cm]
E_a : activation energy [kJ mol^{-1}]
K_{iA} : inhibition constant for oleic acid [mmol L^{-1}]
K_{iB} : inhibition constant for n-butanol [mmol L^{-1}]
K_{mA} : Michaelis constant for oleic acid [mmol L^{-1}]
K_{mB} : Michaelis constant for n-butanol [mmol L^{-1}]
K_{SL} : solid-liquid mass transfer coefficient [cm s^{-1}]
M : molecular weight of the solvent [g mol^{-1}]
R_p : particle radius [cm]
R : ideal gas constant [J $mol^{-1}\ K^{-1}$]
r : Pearson's correlation coefficient
Re_p : Reynolds number
S_0 : initial substrate concentration [mmol L^{-1}]
Sc : Schmidt number
Sh : Sherwood number

T : absolute temperature [K]
u_{pL} : particle velocity relative to the bulk liquid [cm s^{-1}]
V_c : critical volume of oleic acid [cm^3 mol^{-1}]
V_{max} : maximum rate of the reaction [mmol L^{-1} min^{-1}]
V_p : volume of catalyst particle [cm^3]
V_s : molar volume of the solute at the normal boiling point [cm^3 mol^{-1}]
x : association factor of the solvent
ε_p : particle porosity
η : viscosity of the solvent [cP]
η_E : external effectiveness factor
η_I : internal effectiveness factor
μ_L : viscosity of liquid mixtures [g cm^{-1} s^{-1}]
ν : initial reaction rate of esterification [mmol L^{-1} min^{-1}]
ρ_L : density of liquid mixtures [g cm^{-3}]
σ_c : constriction factor
τ : tortuosity factor
Φ : Thiele modulus

REFERENCES

1. M. Hajar and F. Vahabzadeh, *Ind. Crops Prod.*, **52**, 430 (2014).
2. M. Hajar and F. Vahabzadeh, *Ind. Crops Prod.*, **59**, 252 (2014).
3. N. Salih, J. Salimon and E. Yousif, *Ind. Crops Prod.*, **34**, 1089 (2011).
4. J. Salimon, N. Salih and E. Yousif, *Eur. J. Lipid Sci. Technol.*, **112**, 519 (2010).
5. J. H. Lee, S. B. Kim, H. Y. Yoo, J. H. Lee, C. Park, S. O. Han and S. W. Kim, *Korean J. Chem. Eng.*, **30**, 1272 (2013).
6. J. H. Lee, S. B. Kim, H. Y. Yoo, J. H. Lee, S. O. Han, C. Park and S. W. Kim, *Korean J. Chem. Eng.*, **30**, 1335 (2013).
7. H. Ghamgui, M. Karra-Chaabouni and Y. Gargouri, *Enzyme Microb. Technol.*, **35**, 355 (2004).
8. V. M. Balcao, A. L. Paiva and F. X. Malcata, *Enzyme Microb. Technol.*, **18**, 392 (1996).
9. P. M. Doran, *Bioprocess engineering principles*, 2nd Ed., Academic Press (2013).
10. D. D. Do, *Chem. Eng. J.*, **28**, B51 (1984).
11. D. L. Purich, *Enzyme kinetics: Catalysis control: A reference of theory and best-practice methods*, Elsevier (2010).
12. R. R. Lowry and I. J. Tinsley, *J. Am. Oil Chem. Soc.*, **53**, 470 (1976).
13. D. Y. Kwon and J. S. Rhee, *J. Am. Oil Chem. Soc.*, **63**, 89 (1986).
14. L. L. Lapin, *Modern engineering statistics*, Belmont CA, USA, Wadsworth Publishing Company (1997).
15. N. Chaibakhsh, M. B. Abdul Rahman, F. Vahabzadeh, S. Abd-Aziz, M. Basri and A. B. Salleh, *Biotechnol. Bioprocess Eng.*, **15**, 846 (2010).
16. M. Basri, M. A. Kassim, R. Mohamad and A. B. Ariff, *J. Mol. Catal. B: Enzym.*, **85-86**, 214 (2013).
17. M. Hajar, S. Shokrollahzadeh, F. Vahabzadeh and A. Monazzami, *Enzyme Microb. Technol.*, **45**, 188 (2009).
18. A. Zaidi, J. L. Gainer, G. Carta, A. Mrani, T. Kadiri, Y. Belarbi and A. Mir, *J. Biotechnol.*, **93**, 209 (2002).
19. G. D. Yadav and S. Devendran, *Process Biochem.*, **47**, 496 (2012).
20. D. Bezbradica, D. Mijin, S. Siler-Marinkovic and Z. Knezevic, *J. Mol. Catal. B: Enzym.*, **38**, 11 (2006).
21. M. Suchmacher and M. Geller, *Practical biostatistics*, Elsevier (2012).
22. H. W. Blanch and D. S. Clark, *Biochemical Engineering*, Marcel Dekker, New York (1997).
23. C. R. Wilke and P. Chang, *AIChE J.*, **1**, 264 (1955).
24. M. T. Tyn and W. F. Calus, *Processing*, **21**, 16 (1975).
25. K. G. Joback and R. C. Reid, *Chem. Eng. Commun.*, **57**, 233 (1987).
26. J. J. Carberry, *Chemical and catalytic reaction engineering*, McGraw-Hill, New York (1976).
27. H. P. Dong, Y. J. Wang and Y. G. Zheng, *J. Mol. Catal. B: Enzyme.*, **66**, 90 (2010).
28. W. Chulalaksananukul, J. S. Condoret, P. Delorme and R. M. Willemot, *FEBS Lett.*, **276**, 181 (1990).
29. J. Durbin and G. S. Watson, *Biometrika.*, **38**, 159 (1951).
30. M. D. Remero, L. Calvo, C. Alba and A. Daneshfar, *J. Biotechnol.*, **127**, 269 (2007).
31. A. Daneshfar, H. S. Ghaziaskar, L. Shiri, M. H. Manafi, M. Nikorazm and S. Abassi, *Biochem. Eng. J.*, **37**, 279 (2007).
32. C. J. Pouchert and J. Behnke, *The Aldrich Library of ^{13}C and ^{1}H FT NMR Spectra*, Aldrich Chemical Co. (1993).
33. A. Chowdhury, R. Chakraborty, D. Mitra and D. Biswas, *Ind. Crops Prod.*, **52**, 783 (2014).